

# High-Resolution Infrared Spectroscopy of *trans*- and *cis*-H<sup>18</sup>ON<sup>18</sup>O: Equilibrium Structures of the Nitrous Acid Isomers

V. Sironneau,<sup>†</sup> J. Orphal,<sup>\*,†</sup> J. Demaison,<sup>‡</sup> and P. Chelin<sup>†</sup>

Laboratoire Interuniversitaire des Systèmes Atmosphériques (LISA), CNRS UMR 7583, Universités Paris-7 et Paris-12 (Paris-Est), 91405 Créteil Cedex, France, and Laboratoire de Chimie Quantique et Photophysique, CP 160/09, Faculté des Sciences, Université Libre de Bruxelles (ULB), B-1050 Bruxelles, Belgium

Received: July 16, 2008; Revised Manuscript Received: August 29, 2008

In this paper, we present the first high-resolution spectra and analysis of the  $\nu_4$  fundamental bands of fully <sup>18</sup>O-substituted nitrous acid, *trans*- and *cis*-H<sup>18</sup>ON<sup>18</sup>O. These bands are not perturbed by neighboring vibrational levels and were used to determine for the first time accurate rotational and centrifugal distortion constants of the ground and  $\nu_4 = 1$  states of *trans*- and *cis*-H<sup>18</sup>ON<sup>18</sup>O. The ground-state rotational constants were then used, together with the rotational constants of other HONO isotopic species and with rotation–vibration parameters from *ab initio* calculations, to determine accurate semi-experimental equilibrium structures of *trans*- and *cis*-HONO. Our study confirms the results of a recent work by Demaison et al. (*J. Phys. Chem. A* 2006, 110, 13609–13617) concerning the structure of *trans*-HONO, whereas the new structure of *cis*-HONO obtained in this paper is a significant improvement compared with the previous work of Cox et al. (*J. Mol. Struct.* 1994, 320, 91–106). The recommended parameters for the equilibrium structure of *cis*-HONO are  $r_e(\text{O}=\text{N}) = 1.1816(10)$  Å,  $r_e(\text{N}-\text{O}) = 1.3887(10)$  Å,  $r_e(\text{O}-\text{H}) = 0.9744(7)$  Å,  $\angle_c(\text{ONO}) = 113.18(1)^\circ$ , and  $\angle_c(\text{HON}) = 104.67(4)^\circ$ .

## 1. Introduction

Nitrous acid, HONO, is an important atmospheric molecule (see ref 1 and references therein); in particular, it is a significant source for OH radicals in the troposphere, and it is involved in tropospheric HO<sub>x</sub> and NO<sub>x</sub> photochemical processes. Its sources and sinks are not well understood, and *in situ* measurements of HONO using spectroscopic techniques are currently developed (see ref 2 and references therein).

HONO is also interesting for molecular physics and dynamics: it is one of the smallest molecules presenting two isomeric structures, and as early as in 1963, the possibility of photoinduced *trans*–*cis* isomerization has been investigated.<sup>3</sup> This makes HONO very attractive for *ab initio* calculations of molecular dynamics (see refs 4 and 5 and references therein). Nitrous acid exists in two stable planar configurations (*trans* and *cis*),<sup>6</sup> and each isomer has six infrared-active fundamental vibrations. The ground-state rotational and centrifugal distortion constants of the most abundant species, <sup>1</sup>H<sup>16</sup>O<sup>14</sup>N<sup>16</sup>O, are very well established,<sup>7</sup> and there are also several high-resolution studies of the DONO species (see ref 8 and references therein) and of the HO<sup>15</sup>NO species.<sup>6</sup> However, in the latter study by Cox et al.,<sup>6</sup> concerning <sup>18</sup>O-substituted HONO, only the rotational constants of *trans*-H<sup>16</sup>ON<sup>18</sup>O and *trans*-H<sup>18</sup>ON<sup>16</sup>O could be used for the structure determination; in particular, there is complete absence of any high-resolution study of the <sup>18</sup>O-substituted *cis*-HONO species, which is the reason why the equilibrium structure of the *cis*-species is much less accurate than the structure of the *trans*-species.<sup>6,9</sup>

Therefore, following our recent investigations<sup>7,8,10</sup> of HONO and DONO, we decided to attempt recording the high-resolution infrared absorption spectrum of fully <sup>18</sup>O-substituted HONO in

order to determine the ground-state rotational constants of *trans*- and *cis*-H<sup>18</sup>ON<sup>18</sup>O, which would provide new spectroscopic information for an accurate determination of the equilibrium structures of *trans*- and *cis*-HONO.

## 2. Experimental Section

The high-resolution absorption spectrum of fully <sup>18</sup>O-substituted HONO, H<sup>18</sup>ON<sup>18</sup>O, was recorded using the Bruker IFS 125HR (an upgraded IFS 120HR) Fourier-transform spectrometer at the Université de Paris-Est in Créteil. The spectrometer was equipped with a SiC infrared broadband source, with a KBr beam splitter, and with a HgCdTe detector cooled to 77 K. The spectrum covering the 450–6000 cm<sup>-1</sup> region was recorded in 14 blocks of 100 interferometer scans each with a spectral resolution of 0.005 cm<sup>-1</sup>. The absorption cell (installed on top of the sample compartment of the Bruker instrument) is a White-type multipass cell with a base length of 80 cm equipped with CsI windows. The optical path length for the experiments described here was 960 cm. The HONO sample was produced inside the absorption cell using a mixture of N<sup>16</sup>O<sub>2</sub> (about 2 hPa) and H<sub>2</sub><sup>18</sup>O (about 2 hPa); furthermore, pure <sup>18</sup>O<sub>2</sub> (about 15 hPa) was added to the mixture. Due to the pressure, the observed width of the HONO lines is about 0.005 cm<sup>-1</sup>.

Since the goal of this experiment was to perform a line-by-line analysis of the spectra of *trans*- and *cis*-H<sup>18</sup>ON<sup>18</sup>O, it was essential to obtain a pure spectrum of fully <sup>18</sup>O-substituted HONO, without any traces of <sup>16</sup>O-containing HONO. The reason is that, from harmonic force field calculations (see below), we knew that the  $\nu_4$  bands of all <sup>16</sup>O- or <sup>18</sup>O-containing *trans*- and *cis*-HONO species occur in the 780–860 cm<sup>-1</sup> region, so for an isotopic mixture containing both <sup>16</sup>O and <sup>18</sup>O, one would expect an overlap of not less than eight fundamental bands over a range of only 80 cm<sup>-1</sup>, which would be very difficult to resolve

\* Corresponding author. E-mail: orphal@lisa.univ-paris12.fr.

<sup>†</sup> Universités Paris-7 et Paris-12 (Paris-Est).

<sup>‡</sup> Université Libre de Bruxelles (ULB).

**TABLE 1: Rotational and Centrifugal Distortion Constants of the  $\nu_4 = 1$  and Ground States of *trans*- and *cis*-H<sup>18</sup>ON<sup>18</sup>O in the A Reduction of the Watson Hamiltonian (*I<sub>r</sub>* Representation)**

parameter	<i>trans</i> -H <sup>18</sup> ON <sup>18</sup> O		<i>cis</i> -H <sup>18</sup> ON <sup>18</sup> O	
	$\nu_4$	ground state	$\nu_4$	ground state
A (cm <sup>-1</sup> )	3.004 822(16)	2.987 84(82)	2.758 892 6(29)	2.739 25(68)
B (cm <sup>-1</sup> )	0.372 947 63(38)	0.374 884 5(44)	0.389 275 17(77)	0.391 722 9(48)
C (cm <sup>-1</sup> )	0.330 200 70(34)	0.332 537 4(40)	0.339 039 16(67)	0.342 107 9(46)
$\Delta_J$ (10 <sup>-6</sup> cm <sup>-1</sup> )	0.412 488(162)	0.419 39(177)	0.445 84(38)	0.4560(23)
$\Delta_{JK}$ (10 <sup>-6</sup> cm <sup>-1</sup> )	0.761 01(182)	1.3046(187)	-0.8456(34)	-0.3122(195)
$\Delta_K$ (10 <sup>-6</sup> cm <sup>-1</sup> )	105.0610(100)	99.9541 <sup>a</sup>	70.2763(184)	65.3248 <sup>a</sup>
$\delta_J$ (10 <sup>-6</sup> cm <sup>-1</sup> )	0.052 506(132)	0.053 44(103)	0.072 44(30)	0.071 30(127)
$\delta_K$ (10 <sup>-6</sup> cm <sup>-1</sup> )	2.725(28)	2.38(41)	2.557(46)	2.81(41)
$\nu_0$ (cm <sup>-1</sup> )	779.324 264(49)		837.308 478(89)	
$\sigma$ (cm <sup>-1</sup> )	0.000 61	0.000 87	0.000 70	0.000 99
$\Delta$ (amu A <sup>2</sup> )	0.2411	0.0840	0.3062	0.0870
no. of lines	1217	591	1369	769
max <i>J</i> value	41	39	37	37
max <i>K<sub>a</sub></i> value	13	11	13	12

<sup>a</sup> Constant kept fixed to the value of H<sup>16</sup>ON<sup>16</sup>O in ref 7.

**TABLE 2: Rotational and Centrifugal Distortion Constants of the  $\nu_4 = 1$  and Ground States of *trans*- and *cis*-H<sup>18</sup>ON<sup>18</sup>O in the S Reduction of the Watson Hamiltonian (*I<sub>r</sub>* Representation)**

parameter	<i>trans</i> -H <sup>18</sup> ON <sup>18</sup> O		<i>cis</i> -H <sup>18</sup> ON <sup>18</sup> O	
	$\nu_4$	ground state	$\nu_4$	ground state
A (cm <sup>-1</sup> )	3.004 849 8(16)	2.987 87(84)	2.758 670 7(18)	2.739 03(70)
B (cm <sup>-1</sup> )	0.372 942 34(39)	0.374 879 8(45)	0.389 267 11(47)	0.391 717 0(49)
C (cm <sup>-1</sup> )	0.330 206 22(34)	0.332 542 2(42)	0.339 048 54(41)	0.342 114 3(48)
$D_J$ (10 <sup>-6</sup> cm <sup>-1</sup> )	0.401 716(128)	0.409 96(73)	0.431 755(160)	0.441 73(77)
$D_{JK}$ (10 <sup>-6</sup> cm <sup>-1</sup> )	0.827 43(169)	1.3623(179)	-0.737 15(175)	-0.2232(155)
$D_K$ (10 <sup>-6</sup> cm <sup>-1</sup> )	104.9794(99)	99.8803 <sup>a</sup>	70.0642(114)	65.2249 <sup>a</sup>
$d_1$ (10 <sup>-6</sup> cm <sup>-1</sup> )	-0.052 506(141)	-0.053 43(104)	-0.071 798(193)	-0.071 40(131)
$d_2$ (10 <sup>-6</sup> cm <sup>-1</sup> )	-0.005 387(59)	-0.004 70(89)	-0.009 177(80)	-0.007 33(114)
$\nu_0$ (cm <sup>-1</sup> )	779.324 259(49)		837.308 546(55)	
$\sigma$ (cm <sup>-1</sup> )	0.000 61	0.000 87	0.000 70	0.000 99
$\Delta$ (amu A <sup>2</sup> )	0.2396	0.0828	0.3034	0.0850
no. of lines	1217	591	1369	769
max <i>J</i> value	41	39	37	37
max <i>K<sub>a</sub></i> value	13	11	13	12

<sup>a</sup> Constant kept fixed to the value of H<sup>16</sup>ON<sup>16</sup>O in ref 7.

and to analyze at room temperature. It is also important to stress that the only infrared bands that were expected to be free of perturbations due to neighboring vibrational states are the  $\nu_4$  bands, which is indicated both by the harmonic force field calculations (see below) and by the previous analysis<sup>11</sup> of the  $\nu_4$  bands of the most abundant species, *trans*- and *cis*-H<sup>18</sup>ON<sup>18</sup>O.

The presence of <sup>18</sup>O<sub>2</sub> in large excess inside the absorption cell and the use of pure H<sub>2</sub><sup>18</sup>O for the synthesis of HONO did indeed lead to a successful synthesis of *trans*- and *cis*-H<sup>18</sup>ON<sup>18</sup>O. In particular, although there are also some lines of isotopic NO<sub>2</sub> species (N<sup>18</sup>O<sub>2</sub> and N<sup>16</sup>O<sup>18</sup>O), the lines of HONO with single <sup>16</sup>O substitution are significantly weaker than those of pure H<sup>18</sup>ON<sup>18</sup>O, and the lines of H<sup>16</sup>ON<sup>16</sup>O are probably within the noise. One can thus conclude that the isotopic predominance of <sup>18</sup>O-containing species within the absorption cell resulted in a dominant presence of H<sup>18</sup>ON<sup>18</sup>O compared with the <sup>16</sup>O-containing species so that the line-by-line analysis of the two well-separated  $\nu_4$  bands of *trans*- and *cis*-H<sup>18</sup>ON<sup>18</sup>O was feasible.

The line positions were determined using the peakfinder routine of the OPUS software and were calibrated to absolute wavenumbers using H<sub>2</sub><sup>18</sup>O lines from the HITRAN database,<sup>12</sup> and good agreement (a root-mean-square deviation of 0.0007 cm<sup>-1</sup> between the observed and reference line positions) was observed after the calibration.

### 3. Rotational Analysis

The rotational assignments and analysis of the  $\nu_4$  fundamental bands of both species were rather straightforward, although no ground-state constants were known for *trans*- and *cis*-H<sup>18</sup>ON<sup>18</sup>O. Therefore, as a first step, the harmonic force field of *trans*- and *cis*-HONO was calculated with the ASYM20 code written by Hedberg and Mills<sup>13</sup> using the known infrared band centers of several HONO isotopic species including (DONO, HO<sup>15</sup>NO), and in this way, the centers of the  $\nu_4$  fundamental bands of *trans*- and *cis*-H<sup>18</sup>ON<sup>18</sup>O and their ground-state rotational constants (including the harmonic contributions to the vibrational dependence of the rotational constants) were calculated. The predicted band centers of the  $\nu_4$  fundamental bands of *trans*- and *cis*-H<sup>18</sup>ON<sup>18</sup>O are, respectively, 780.3 and 835.6 cm<sup>-1</sup> (to compare with the observed band centers in Tables 1 and 2), thus indicating that the observed bands can indeed be attributed to the fully <sup>18</sup>O-substituted nitrous acid isomers. As for the most abundant species H<sup>16</sup>ON<sup>16</sup>O analyzed previously,<sup>11</sup> the  $\nu_4$  fundamental band of the *cis*-isomer is observed to be higher in energy than the  $\nu_4$  band of the *trans*-isomer.

To start with the rotational analysis, the ground-state rotational constants predicted from the harmonic force fields were then corrected for the anharmonic contributions using the ratio of the ground-state rotational constants of the normal HONO

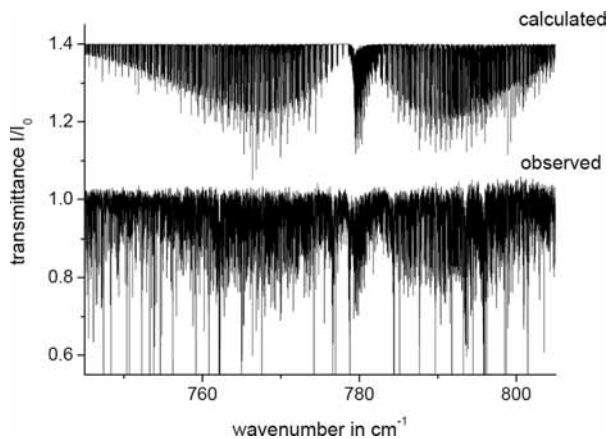


**Figure 1.** Overview of the  $\nu_4$  band of *trans*-H<sup>18</sup>ON<sup>18</sup>O at high resolution. The upper plot shows the synthetic spectrum (shifted upward for clarity) obtained using the rotational and centrifugal distortion constants obtained in this study; the lower plot shows the experimental spectrum. Note that all lines are well resolved. Strong lines in the experimental spectrum that are not reproduced by the synthetic spectrum are due to H<sub>2</sub>O and isotopic NO<sub>2</sub> species (N<sup>18</sup>O<sub>2</sub> and N<sup>16</sup>O<sup>18</sup>O).

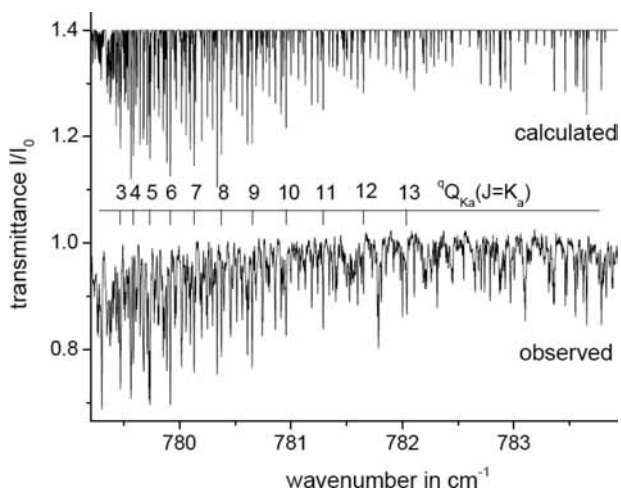


**Figure 2.** Expanded view of the  $Q$ -branch of the  $\nu_4$  band of *trans*-H<sup>18</sup>ON<sup>18</sup>O. Again, there are some lines due to H<sub>2</sub>O and isotopic NO<sub>2</sub> species (N<sup>18</sup>O<sub>2</sub> and N<sup>16</sup>O<sup>18</sup>O) in the experimental spectrum that are not reproduced in the synthetic spectrum. There is good agreement between the calculated and observed spectrum concerning the HONO lines.

species (*trans*- and *cis*-H<sup>16</sup>ON<sup>16</sup>O) from experiment<sup>7</sup> and from the harmonic force field calculated in this study. To have a first prediction of the rotational constants in the  $\nu_4 = 1$  states, the

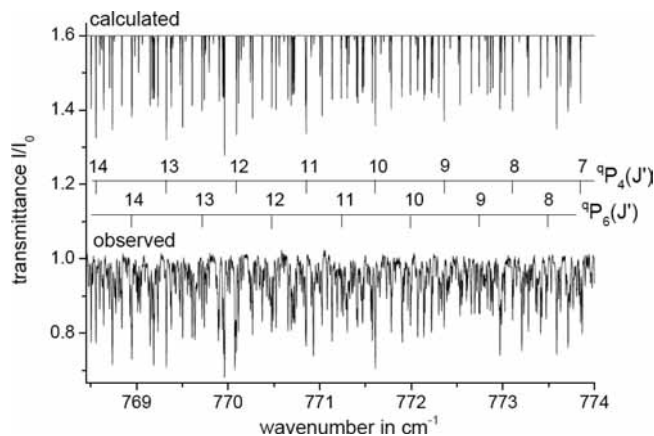


**Figure 3.** Part of the  $P$ -branch of the  $\nu_4$  band of *trans*-H<sup>18</sup>ON<sup>18</sup>O. See also comments for Figure 2.

vibrational dependence of the rotational constants was estimated using the rotational analysis of the  $\nu_4$  bands of *trans*- and *cis*-H<sup>16</sup>ON<sup>16</sup>O published previously.<sup>11</sup> With these constants, first synthetic spectra of the  $\nu_4$  bands of *trans*- and *cis*-H<sup>18</sup>ON<sup>18</sup>O were calculated. Note that all calculations of this study were made with a Watson-type Hamiltonian<sup>14</sup> in the  $A$ - and  $S$ -reductions ( $I'$  representation).

Although the spectrum is contaminated by strong lines of isotopic NO<sub>2</sub> species (N<sup>18</sup>O<sub>2</sub> and N<sup>16</sup>O<sup>18</sup>O), in particular in the region of the  $\nu_4$  band of *trans*-H<sup>18</sup>ON<sup>18</sup>O (see Figure 1), the line-by-line assignments of HONO were rather straightforward: after first assignments in the  $Q$  branches (see Figure 2), some lines with low values of the  $J$  and  $K_a$  quantum numbers were identified in the  $P$ - and  $R$ -branches, leading to a first set of rotational constants, which were used for new predictions. This procedure comprising new line assignments and least-squares fits of the rotational constants followed by new line predictions was repeated until all strong isolated lines in the  $\nu_4$  bands were assigned (see, for example, Figure 3). Figure 4 shows an overview of the  $\nu_4$  band of *cis*-H<sup>18</sup>ON<sup>18</sup>O, and Figure 5 shows the  $Q$ -branch region of this band.

The final results of the rotational analysis are given in Tables 1 and 2. In the final calculations, 1217 observed infrared lines of *trans*-H<sup>18</sup>ON<sup>18</sup>O and 1369 observed infrared lines of *cis*-H<sup>18</sup>ON<sup>18</sup>O were included; the root-mean-square deviations between the observed and calculated line positions are 0.000 68 cm<sup>-1</sup> for *trans*-H<sup>18</sup>ON<sup>18</sup>O and 0.000 70 cm<sup>-1</sup> for *cis*-H<sup>18</sup>ON<sup>18</sup>O. These results are very similar to the previous analysis<sup>11</sup> of the  $\nu_4$  bands of *trans*- and *cis*-H<sup>16</sup>ON<sup>16</sup>O indicating good quality

**TABLE 3: Molecular Structure of *cis*-HONO with Distances ( $r$ ) in Å and Angles ( $\angle$ ) in Degrees**

method <sup>a</sup>	basis set <sup>b</sup>	$r(\text{O}=\text{N})$	$r(\text{N}-\text{O})$	$r(\text{O}-\text{H})$	$\angle(\text{ONO})$	$\angle(\text{HON})$
CCSD(T) fc	VTZ	1.1874	1.3915	0.9765	113.14	104.03
CCSD(T) fc	VQZ	1.1841	1.3863	0.9750	113.22	104.52
MP2 fc	VQZ	1.1888	1.3786	0.9771	113.29	104.44
MP2 fc	V5Z	1.1883	1.3779	0.9773	113.30	104.66
MP2 fc	augVQZ	1.1889	1.3799	0.9781	113.32	104.70
MP2 fc	wCVQZ	1.1886	1.3779	0.9773	113.29	104.46
MP2 ae	wCVQZ	1.1867	1.3743	0.9765	113.34	104.56
$r_e^c$		1.1816	1.3820	0.9743	113.27	104.84
$r_e(\text{se})^d$		1.1823(25)	1.3880(26)	0.9741(13)	113.19(4)	104.71(16)
$r_e(\text{se})^e$		1.1816(10)	1.3887(10)	0.9744(7)	113.18(1)	104.67(4)
$r_d^f$		1.190(5)	1.397(6)	0.975(3)	113.5(3)	104.4(4)

<sup>a</sup> fc = frozen core approximation; ae = all electrons correlated. <sup>b</sup> VnZ = cc-pVnZ; AVQZ = aug-cc-p-VQZ. <sup>c</sup> CCSD(T)/VQZ + MP2(fc)[V5Z - VQZ] + MP2[wCVQZ(ae) - wCVQZ(fc)]. <sup>d</sup> Semi-experimental structure, all parameters free; see text. <sup>e</sup> Semi-experimental structure with  $r_e(\text{O}=\text{N}) = 1.1816(10)$  Å fixed; see text. <sup>f</sup> Zero-point average structure from ref 6.

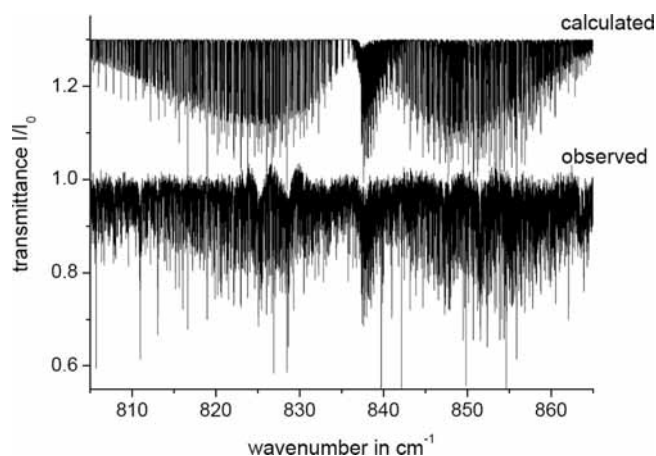


**Figure 4.** Overview of the  $\nu_4$  band of *cis*-H<sup>18</sup>ON<sup>18</sup>O at high resolution. The upper plot shows the synthetic spectrum (shifted upward for clarity) obtained using the rotational and centrifugal distortion constants obtained in this study; the lower plot shows the experimental spectrum. Note that all lines are well resolved. The  $\nu_4$  band of *cis*-H<sup>18</sup>ON<sup>18</sup>O is slightly weaker than the  $\nu_4$  band of *trans*-H<sup>18</sup>ON<sup>18</sup>O, as also observed for the normal species H<sup>16</sup>ON<sup>16</sup>O. Note some small baseline problems due to fringes in the 825–830 cm<sup>-1</sup> region.

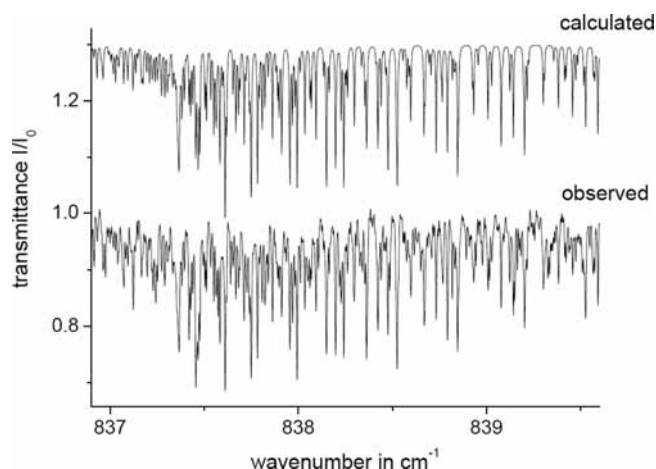


**Figure 5.** Expanded view of the *Q*-branch of the  $\nu_4$  band of *cis*-H<sup>18</sup>ON<sup>18</sup>O. Note the good agreement between the calculated and observed spectrum concerning the HONO lines.

also for the lower state rotational and centrifugal distortion constants that were determined using ground-state combination differences. The *S*-reduction provides slightly better fits as indicated by the reduction<sup>14</sup> parameters  $s_{111}$  (which is the coefficient of the unitary transformation operator used to reduce the Hamiltonian;<sup>14</sup> it should be as small as possible in order to ensure good convergence of the calculations). Note also that only five of the six centrifugal distortion constants could be determined for the ground states, and the  $\Delta_K$  (or  $D_K$ ) constants were constrained in the least-squares calculations to the values of the main isotopic species H<sup>16</sup>ON<sup>16</sup>O published previously<sup>7</sup> and compared with the estimations from the harmonic force fields and *ab initio* calculations, in order to avoid any systematic errors that might influence the structure calculations (see below).

#### 4. Equilibrium Structures

**4.1. Structure of *trans*-HONO.** Because the rotational constants of H<sup>18</sup>ON<sup>18</sup>O are determined for the first time, it is tempting to recalculate a semiexperimental equilibrium structure of *trans*-HONO to see whether these rotational constants

improve the fit. Actually, the addition of these new data decreases neither the standard deviation of the parameters nor the condition number.<sup>15</sup> Furthermore, the parameters are left unchanged. This confirms the accuracy of the parameters determined in ref 9.

**4.2. *Ab Initio* Structure of *cis*-HONO.** The geometry of *cis*-HONO was first optimized *ab initio* at the coupled cluster level of theory with single and double excitations (CCSD)<sup>16</sup> augmented by a perturbational estimate of the effects of connected triple excitations [CCSD(T)].<sup>17</sup> The MOLPRO suite of programs was used.<sup>18</sup> Unless otherwise mentioned, the frozen core (fc) approximation was used, that is, only the valence electrons were included in the correlation treatment. Dunning's correlation-consistent polarized basis sets,<sup>19</sup> cc-pVXZ, with X = T, Q, were used.

The small effect of basis set enlargement beyond quadruple- $\zeta$  was tested with the cc-pV5Z basis set using the second-order Møller–Plesset perturbation theory (MP2).<sup>20</sup> The effect of including diffuse functions was tested using the augmented quadruple- $\zeta$  basis set (aug-cc-pVQZ)<sup>21</sup> at the MP2 level of theory. Finally, to estimate the core correlation, the weighted core-valence quadruple- $\zeta$  basis set (cc-pwCVQZ)<sup>22</sup> was employed at the MP2 level of theory. For the calculation of these small corrections, the use of the cheaper MP2 method is justified by the fact that it gives almost identical results as the CCSD(T) method, at least for first-row atoms. This was in particular checked for *trans*-HONO.<sup>9</sup>

The results are reported in Table 3. The coupled cluster  $T_1$  diagnostic value<sup>23</sup> is 0.021 at the CCSD(T)/cc-pVQZ level. This is the same value as for *trans*-HONO, and it is slightly larger than the usual cutoff value, 0.020. This suggests that the CCSD(T) method is not fully reliable as was previously found for *trans*-HONO. In particular, the CCSD(T) value of the length of the long N–O bond is expected to be too short by about 0.008 Å (*trans*-HONO value). Going from cc-pVQZ to cc-pV5Z, all bond lengths remain almost unaffected: O=N and N–O decrease by 0.0006 and 0.0007 Å, respectively, while O–H increases by 0.0002 Å. The angle  $\angle(\text{HON})$  increases by 0.215°, while the  $\angle(\text{ONO})$  angle increases by only 0.012°. This behavior is almost identical to that found for *trans*-HONO, and it may be concluded that convergence of the geometrical parameters of HONO within the cc-pVXZ series is almost achieved with the cc-pVQZ basis set.

The inclusion of diffuse functions (at the aug-cc-pVQZ level) increases the N–O bond length by only 0.0013 Å and is almost negligible for the other parameters. It is known<sup>24,25</sup> that the effect of diffuse functions rapidly decreases with the size of the basis set; thus it should be completely negligible at the cc-pV5Z level. Core correlation effects have the expected order of magnitude leading to a decrease of 0.0019, 0.0036, and 0.0008 Å for the N=O, N–O, and O–H bond lengths, respectively. Adding the core corrections as well as the small corrections, cc-pVQZ  $\rightarrow$  cc-pV5Z, to the valence-only CCSD(T)/cc-pVQZ values gives an estimate of the equilibrium structure of *cis*-HONO.

In *cis*-HONO,  $r(\text{O–H})$  is 0.009 Å longer than that in *trans*-HONO (0.9743 Å compared with 0.9651 Å). This is in perfect agreement with the variation of the  $\nu(\text{OH})$  stretching frequency.<sup>26</sup> This indicates that the *ab initio* value of this bond length is reliable.

**4.3. Semi-experimental Structure of *cis*-HONO.** The anharmonic force field of HONO was calculated with the Kohn–Sham density functional theory<sup>27</sup> using Becke's three-parameter hybrid exchange functional<sup>28</sup> and the Lee–Yang–Parr correlation functional,<sup>29</sup> together denoted as B3LYP. These

**TABLE 4: Semi-experimental Equilibrium Rotational Constants (MHz) of *cis*-HONO**

	A	B	C
HONO			
se <sup>a</sup>	84145.20	13341.290	11516.000
o-c <sup>b</sup>	-0.16	-0.414	0.190
DONO			
se	70947.27	13060.740	11030.770
o-c	-8.28	-0.274	0.190
HO <sup>15</sup> NO			
se	80738.07	13335.270	11446.420
o-c	-43.59	-0.273	0.401
H <sup>18</sup> ON <sup>18</sup> O			
se	82158.21	11892.170	10389.340
o-c	-24.78	-0.338	0.218

<sup>a</sup> Semi-experimental equilibrium rotational constant, that is, experimental ground-state constants corrected by *ab initio*  $\alpha$ -constants. <sup>b</sup> Residuals of rotational constants from least-squares fit.

calculations were performed with the TZ2Pf basis set, a valence triple- $\zeta$  plus double polarization plus *f* function basis set.<sup>30</sup> This B3LYP/TZ2Pf level of theory was chosen because it was found to give the best results for *trans*-HONO. For these computations, the Gaussian03 program was utilized.<sup>31</sup>

The vibration-rotation interaction constants deduced from the B3LYP force field were combined with the experimental ground-state rotational constants to yield the semi-experimental equilibrium rotational constants. These constants were corrected for a small electronic effect using the experimental *g*-constants.<sup>32</sup> This correction is too small to significantly affect the final structure. However, it decreases (in absolute value) the equilibrium inertial defect, which is almost 2 orders of magnitude smaller than the ground-state inertial defect ( $\Delta_e = -0.0019 \text{ u}\text{\AA}^2$  to be compared with  $\Delta_0 = 0.0850 \text{ u}\text{\AA}^2$  for the parent isotopologue), indicating that the equilibrium rotational constants are reliable. The semi-experimental equilibrium rotational constants are given in Table 4. The semi-experimental structure was calculated using the iteratively reweighted least-squares method,<sup>33</sup> as for *trans*-HONO. A first fit whose results are given in the second last line of Table 3 gave parameters in good agreement with the *ab initio* structure, except, as expected, for the  $r_e(\text{N}-\text{O})$  bond length whose *ab initio* value is obviously too short as in *trans*-HONO. However, the fit is not well conditioned; the condition number is as large as 439 and the  $r_e(\text{O}=\text{N})$  and  $r_e(\text{N}-\text{O})$  bond lengths are highly correlated. For this reason, the standard deviations of the parameters are rather large. To avoid this problem, we have repeated the fit fixing  $r_e(\text{O}=\text{N})$  at its *ab initio* value with an uncertainty of 0.001 Å. The result of the fit is given in the second last line of Table 3. It is in good agreement with the preceding fit, but the standard deviations are significantly smaller, and the condition number is reduced to 22.8 indicating that all parameters are well determined. It is worth noting that, as for *trans*-HONO, the CCSD(T) method seems to deliver an accurate structure except for the long  $r(\text{N}-\text{O})$  bond length. This work provides further evidence that the best method to determine the accurate equilibrium structure of a small polyatomic molecule is the semi-experimental technique.

It is interesting to compare this structure with that of the *trans* conformer whose values are<sup>9</sup>  $r_e(\text{O}=\text{N}) = 1.1686(1) \text{ \AA}$ ,  $r_e(\text{N}-\text{O}) = 1.4258(1) \text{ \AA}$ ,  $r_e(\text{O}-\text{H}) = 0.9651(3) \text{ \AA}$ ,  $\angle_e(\text{ONO}) = 110.654(4)^\circ$ , and  $\angle_e(\text{HON}) = 102.035(22)^\circ$ . With the exception of the  $r_e(\text{N}-\text{O})$  bond length, the values of all the

parameters are larger in the *cis* form than in the *trans* form. However, because the  $r_e(\text{N}-\text{O})$  bond length is significantly shorter in the *cis* form (1.389 Å compared with 1.426 Å), the H and end O atoms are close, their distance, 2.106 Å, being slightly shorter than the sum of the van der Waals radii of the H and O atoms (2.160 Å). For this reason, although the bond angles are larger in the *cis* form, it is not possible to exclude the existence of a weak internal hydrogen bond.

## 5. Conclusions

The infrared absorption spectrum of the  $\nu_4$  fundamental bands of fully <sup>18</sup>O-substituted nitrous acid, *trans*- and *cis*-H<sup>18</sup>ON<sup>18</sup>O, was recorded using a high-resolution Fourier-transform spectrometer. The rotational analysis of these bands provided for the first time rotational constants of both species that were used to determine for the first time an accurate semi-experimental equilibrium structure of *cis*-HONO and to confirm the previously determined<sup>9</sup> equilibrium structure of *trans*-HONO.

**Acknowledgment.** This work was performed within the European Associated Laboratory (LEA) “HiRes” and the EU-funded project “QUASAAR” (MRTN-CT-2004-512202). Dr. Demaison is indebted to ULB for providing an invited international chair to him (2006). Part of this work was supported by the French National Programme of Atmospheric Chemistry (LEFE-CHAT). The authors thank Drs. A. G. Maki and W. J. Lafferty for the ASYMBD87 Fortran code used to calculate and fit rotational energy levels (using Watson-type Hamiltonians) and Drs. L. Hedberg and I. M. Mills for the ASYM20 Fortran code used for the harmonic force field calculations.

## References and Notes

- (1) Li, S.; Mathews, J.; Sinha, A. *Science* **2008**, *319*, 1657.
- (2) Gherman, T.; Venables, D. S.; Vaughan, S.; Orphal, J.; Ruth, A. A. *Environ. Sci. Technol.* **2008**, *42*, 890.
- (3) Hall, R. T.; Pimentel, G. C. *J. Chem. Phys.* **1963**, *38*, 1889.
- (4) Luckhaus, D. *J. Chem. Phys.* **2003**, *118*, 8797.
- (5) Richter, F.; Hochlaf, M.; Rosmus, P.; Gatti, F.; Meyer, H.-D. *J. Chem. Phys.* **2004**, *120*, 1306.
- (6) Cox, A. P.; Ellis, M. C.; Atfield, C. J.; Ferris, A. C. *J. Mol. Struct.* **1994**, *320*, 91.
- (7) Dehayem-Kamadjeu, A.; Pirali, O.; Orphal, J.; Kleiner, I.; Flaud, P.-M. *J. Mol. Spectrosc.* **2005**, *234*, 182.
- (8) Dehayem-Kamadjeu, A.; Orphal, J.; Ibrahim, N.; Kleiner, I.; Bouba, O.; Flaud, J.-M. *J. Mol. Spectrosc.* **2006**, *238*, 41.
- (9) Demaison, J.; Csaszar, A. G.; Dehayem-Kamadjeu, A. *J. Phys. Chem. A* **2006**, *110*, 13609.
- (10) Perrin, A.; Miljanic, S.; Dehayem-Kamadjeu, A.; Chelin, P.; Orphal, J.; Demaison, J. *J. Mol. Spectrosc.* **2007**, *245*, 100.
- (11) Kleiner, I.; Guilmot, J. M.; Carleer, M.; Herman, M. *J. Mol. Spectrosc.* **1991**, *149*, 341.
- (12) Rothman, L. S.; Jacquemart, D.; Barbe, A.; Benner, D. C.; Birk, M.; Brown, L. R.; Carleer, M. R.; Chackerian, C., Jr.; Chance, K. V.; Dana, V.; Devi, V. M.; Flaud, J.-M.; Gamache, R. R.; Goldman, A.; Hartmann, J.-M.; Jucks, K. W.; Maki, A. G.; Mandin, J.-Y.; Massie, S.; Orphal, J.; Perrin, A.; Rinsland, C. P.; Smith, M. A. H.; Toth, R. A.; Vander Auwera, J.; Varanasi, P.; Wagner, G. *J. Quant. Spectrosc. Radiat. Transfer* **2005**, *96*, 139.
- (13) Hedberg, L.; Mills, I. M. *J. Mol. Spectrosc.* **1993**, *160*, 117.
- (14) Watson, J. K. G. In *Vibrational Spectra and Structure*; Durig, J. R., Ed.; Elsevier: Amsterdam, 1977; pp 1–89.
- (15) Belsley, D. A. *Conditioning Diagnostics*; Wiley: New York, 1991.
- (16) Purvis, G. D., III; Bartlett, R. J. *J. Chem. Phys.* **1982**, *76*, 1910.
- (17) Raghavachari, K.; Trucks, G. W.; Pople, J. A.; Head-Gordon, M. *Chem. Phys. Lett.* **1989**, *157*, 479.
- (18) MOLPRO 2000 is a package of *ab initio* programs written by Werner, H.-J. and Knowles, P. J. with contributions from Amos, R. D.; Bernhardsson, A.; Berning, A.; Celani, P.; Cooper, D. L.; Deegan, M. J. O.; Dobbyn, A. J.; Eckert, F.; Hampel, C.; Hetzer, G.; Korona, T.; Lindh, R.; Lloyd, A. W.; McNicholas, S. J.; Manby, F. R.; Meyer, W.; Mura, M. E.; Nicklass, A.; Palmieri, P.; Pitzer, R.; Rauhut, G.; Schütz, M.; Stoll, H.; Stone, A. J.; Tarroni, R.; Thorsteinsson, T.
- (19) Dunning, T. H., Jr. *J. Chem. Phys.* **1989**, *90*, 1007.

- (20) Møller, C.; Plesset, M. S. *Phys. Rev.* **1934**, *46*, 618.
- (21) Kendall, R. A.; Dunning, T. H., Jr.; Harrison, R. J. *J. Chem. Phys.* **1992**, *96*, 6796.
- (22) Peterson, K. A.; Dunning, T. H., Jr. *J. Chem. Phys.* **2002**, *117*, 10548.
- (23) Lee, T. J.; Taylor, P. R. *Int. J. Quantum Chem. Symp.* **1989**, *23*, 199.
- (24) Demaison, J. *Mol. Phys.* **2007**, *105*, 3109.
- (25) Kohn, W.; Sham, L. J. *Phys. Rev. A* **1965**, *140*, 1133.
- (26) Demaison, J.; Herman, M.; Liévin, J. *Int. Rev. Phys. Chem.* **2007**, *26*, 391.
- (27) Kohn, W.; Sham, L. J. *Phys. Rev. A* **1965**, *140*, 1133.
- (28) Becke, A. D. *J. Chem. Phys.* **1993**, *98*, 5648.
- (29) Lee, C. T.; Yang, W. T.; Parr, R. G. *Phys. Rev. B* **1988**, *37*, 785.
- (30) Dunning, T. H., Jr. *J. Chem. Phys.* **1971**, *55*, 716.
- (31) Frisch, M. J.; Trucks, G. W.; Schlegel, H. B.; Scuseria, G. E.; Robb, M. A.; Cheeseman, J. R.; Montgomery, J. A., Jr.; Vreven, T.; Kudin, K. N.; Burant, J. C.; Millam, J. M.; Iyengar, S. S.; Tomasi, J.; Barone, V.; Mennucci, B.; Cossi, M.; Scalmani, G.; Rega, N.; Petersson, G. A.; Nakatsuji, H.; Hada, M.; Ehara, M.; Toyota, K.; Fukuda, R.; Hasegawa, J.; Ishida, M.; Nakajima, T.; Honda, Y.; Kitao, O.; Nakai, H.; Klene, M.; Li, X.; Knox, J. E.; Hratchian, H. P.; Cross, J. B.; Adamo, C.; Jaramillo, J.; Gomperts, R.; Stratmann, R. E.; Yazyev, O.; Austin, A. J.; Cammi, R.; Pomelli, C.; Ochterski, J. W.; Ayala, P. Y.; Morokuma, K.; Voth, G. A.; Salvador, P.; Dannenberg, J. J.; Zakrzewski, V. G.; Dapprich, S.; Daniels, A. D.; Strain, M. C.; Farkas, Ö.; Malick, D. K.; Rabuck, A. D.; Raghavachari, K.; Foresman, J. B.; Ortiz, J. V.; Cui, Q.; Baboul, A. G.; Clifford, S.; Cioslowski, J.; Stefanov, B. B.; Liu, G.; Liashenko, A.; Piskorz, P.; Komáromi, I.; Martin, R. L.; Fox, D. J.; Keith, T.; Al-Laham, M. A.; Peng, C. Y.; Nanayakkara, A.; Challacombe, M.; Gill, P. M. W.; Johnson, B.; Chen, W.; Wong, M. W.; Gonzalez, C.; Pople, J. A. *Gaussian03*, Revision B.04; Gaussian Inc.: Wallingford, CT, 2004.
- (32) Hübner, D.; Sutter, D. H. Z. *Naturforsch. A* **1984**, *39*, 55.
- (33) Hamilton, L. C. *Regression with Graphics*; Duxbury Press: Belmont, CA, 1992.

JP806286P